

No observational constraints from hypothetical collisions of hypothetical dark halo primordial black holes with galactic objects

Marek A. Abramowicz^{1,2}, Julia K. Becker¹, Peter L. Biermann^{3,4,5,6,7}
Antonella Garzilli¹, Fredrik Johansson^{1,8} and Lei Qian⁹

ABSTRACT

The possible contribution of primordial black holes (PBHs) to the dark matter in the Universe has been discussed in various ways, implying consequences for observational astronomy. In this paper, we investigate probabilities and possible observational signatures of hypothetical collisions of PBHs with main sequence stars, red giants, white dwarfs, and neutron stars in our Galaxy. This has previously been discussed to lead to an observable photon eruption due to the shock produced in the passage. We find that such collisions are either too rare to be observed if masses of PBHs are typically larger than about 10^{20} g, or they produce too little power to be detected if the PBHs masses are smaller than about 10^{20} g. Apart from signals from those interactions, the only methods to probe their existence are the observation of their evaporation of the PBHs at masses of $m_{pbh} \sim 10^{15}$ g and micro-lensing at masses around $> 10^{26}$ g. Thus, the mass region between 10^{15} g $< m_{pbh} < 10^{25}$ g remains unexplored and leaves space for some contribution of PBHs to the dark matter.

Subject headings: cosmology: dark matter — cosmology: early Universe — Galaxy: abundances — X-rays: bursts — gamma-rays: bursts

1. Introduction

The idea of dark matter in the Universe was first established in the 1930th, when Zwicky (1933, 1937) discussed the deviation of masses of clusters of galaxies from the expected values. Until today,

¹Göteborgs Universitet, Institutionen för Fysik, SE-41296 Göteborg, Sweden

²N. Copernicus Astronomical Centre, Polish Academy of Sciences, Bartycka 18, 00-716 Warszawa

³Max Planck Institut für Radioastronomie, Auf dem Hügel 69, D-53121 Bonn, Germany

⁴Department of Physics and Astronomy, University of Bonn, Germany

⁵Department of Physics and Astronomy, University of Alabama, Tuscaloosa, AL, USA

⁶Department of Physics and Astronomy, University of Alabama, Huntsville, AL, USA

⁷Inst. Nucl. Phys. FZ, Karlsruhe Inst. of Techn. (KIT), Karlsruhe, Germany

⁸Chalmers tekniska högskola, Institutionen för fundamental fysik, SE-41296 Göteborg, Sweden

⁹Astronomy Department, School of Physics, Peking University, Beijing 100871, P. R. China

this idea has been confirmed in many different ways (Ostriker et al. 1974; Komatsu et al. 2008, e.g.). The strong deviation of the rotation curves of spiral galaxies from what is expected from luminous matter was an additional, important, quantitative proof for the existence of dark matter (DM). In particular, the dark matter contents in the Galaxy was first discussed in Kahn and Woltjer (1959), and is today determined to $M_{DM} = 9 \cdot 10^{11} M_{\odot}$ (Xue et al. 2008). Searches for non-luminous, baryonic dark matter like brown and white dwarfs as well as neutron stars, and also black holes as non-baryonic DM at masses above $0.1 - 0.2 \cdot M_{\odot}$ (“Machos”) showed that those objects are far too rare to make up a significant part of the dark matter (Afonso et al. 2003; Yoo et al. 2004). Within the past five years, it was even shown by WMAP that baryonic matter only makes up $\sim 4\%$, while dark matter makes up $\sim 20\%$ of the critical density of the Universe. While objects like neutron stars or white dwarfs are thereby excluded, black holes at masses between $10^{15} \text{ g} < m_{pbh} < 10^{26} \text{ g}$ can still be responsible for a significant fraction as explained in the next section. Those primordial black holes (PBHs) are predicted to be produced in early phases of the Universe due to density fluctuations as observed in the cosmic microwave background. The gravitational radius r_g of those PBHs is subatomic, $r_g \sim 10^{-8} \cdot (m_{pbh}/(10^{20} \text{ g})) \text{ cm}$. The Bondi-Hoyle radius, on the other hand, can be typically significantly larger.

In this paper, we investigate the hypothesis that PBHs represent a fraction of the DM in the Galaxy by considering PBH collisions with Galactic objects. We show that the collisions of the PBHs as discussed by Zhilyaev (2007) would produce no signatures that could be observed at present, even with the most optimistic parameter sets. For alternative approaches to explain dark matter by e.g. the extension of the standard model of particle physics to new particles, see e.g. Haber and Kane (1985); Bertone et al. (2005); Biermann and Kusenko (2006); Hooper and Profumo (2007).

In order to investigate the interaction of PBHs with objects in the Galaxy and possible observational consequences, we need to ask the following questions:

1. *How frequent are the events?*
2. *How energetic is a single event?*
3. *What are possible signatures?*

In the following sections, we answer each question separately for the five most important object classes in the Galaxy, i.e. main sequence stars, red giants (in particular their dense cores), white dwarfs and neutron stars. The main intrinsic properties of those objects are listed together with their abundance in the Galaxy in table 1. Both the interaction probability and the energy loss strongly depend on the listed properties. In addition, we consider a collision with Earth in order to investigate the claim of the Tungus event being of such origin, see Jackson and Ryan (1973).

This paper is organized as follows. Section 3 summarizes the observational constraints that exist presently and Section 2 discusses why we can consider PBHs as approximately uncharged. In Section 4, interaction probabilities are derived. The energy loss of PBH collisions with different classes of Galactic objects is discussed in Section 5. Possible signatures and the detectability of

such events are investigated in Section 6. Section 7 summarizes the conclusions to be drawn from our calculation and discusses further possibilities for detection requiring additional assumptions.

2. Primordial black holes - basic properties

A stationary black hole is fully characterized by its mass, charge and angular momentum. As discussed above, the mass range we consider here is $\sim 10^{15} \text{ g} < m_{pbh} < 10^{26} \text{ g}$. In this section, we investigate the possibility of the PBHs to be significantly charged. This is only important for charges where the electromagnetic force exceeds the gravitational force. The angular momentum becomes important and contributes to energy loss effects through the induction of currents if this charge is significantly large. As we will show here, charge can be neglected and therefore the question of the PBHs angular momentum is not essential in this context.

A PBH may become charged when a small particle with non-zero mass and charge, like a proton or an electron, gets to within a distance of the Bondi-Hoyle radius, r_{Bo-Ho} , of the PBH Bondi and Hoyle (1944):

$$r_{Bo-Ho} = \frac{G \cdot m_{PBH}}{v_{\star}^2} \approx 0.01 \text{ cm} \cdot \left(\frac{m_{pbh}}{10^{20} \text{ g}} \right) \cdot \left(\frac{v_{\star}}{v_0} \right)^{-2} \gg a_{dust}. \quad (1)$$

This assumes that the PBH is supersonic and super-Alfvénic. If that is not the case, the thermal velocity or the Alfvén velocity needs to be applied. The Bondi-Hoyle radius is therefore much larger than the typical grain size, $a_{dust} \sim \mu\text{m}$, see e.g. Mathis et al. (1977); Biermann and Harwit (1980); Yan et al. (2004).

The corresponding radius for charged particle interaction in cgs units is

$$r_{Bo-Ho} = \frac{e^2 Z_{BH} Z}{v_{\star}^2 m_{p,e}}, \quad (2)$$

where Z_{BH} is the charge of the PBH, Z is the charge of the particle, usually unity, but of either sign ($Z = \pm 1, 2, 3, \dots$), and $m_{p,e}$ is the mass of a proton, or electron, depending on which case is under consideration. The combined effect is then

$$r_{Bo-Ho} = \frac{G \cdot m_{PBH} \cdot m_{p,e} - e^2 Z_{BH} Z}{v_{\star}^2 m_{p,e}}. \quad (3)$$

For instance, a PBH, positively charged by unity, attracts electrons and the electric attraction is larger than the gravitation attraction for a PBH of $m_{pbh} = 10^{15} \text{ g}$. This cancels the positive charge relatively quickly. For $Z_{BH} = 100$, the repulsion for protons would exactly cancel the gravitational attraction. So for $Z_{BH} < 100$ the gravitational attraction would dominate over the electric repulsion, and accretion might continue. Thus, a charge of $Z_{BH} = 100$ may be reasonable.

If the charge were negative, then the repulsion for electrons would dominate, and there would be no electron accretion at all. But if the charge were negative, at a level of $Z_{BH} = -100$, and

we consider the attraction for protons, then the attraction would be strong and again cancel the negative charge.

For a PBH with a mass of $m_{pbh} \sim m_p/m_e \cdot 10^{15}$ g, these aspects would scale up. For the general picture the charge is minuscule, and certainly not enough to have any appreciable effect at all.

If the matter is degenerate, then only the particles at the Fermi-surface are available for interaction, and so interaction is strongly reduced.

In white dwarfs for instance the electrons are degenerate and thus not available for interaction, but the protons are. Therefore, one might argue, that traversing PBHs could accumulate arbitrarily large positive charges. However, this accretion is very soon extremely limited because of the repulsion between a positively charged PBH and a proton inside a white dwarf. Even reducing the cross section to basically the hadronic cross section would still give the PBH a huge positive charge. On the other hand, this would happen only to a minuscule fraction of all PBHs.

The interaction may become important at a surface of discontinuity, like coming out of the Fermi-sea of neutrons in a neutron star, and emerging into the gas surrounding it.

However, there are charged dust particles, and applying the same approach as above, the limiting charge for the PBH is then

$$Z_{BH} = \frac{G \cdot m_{PBH} \cdot m_d}{e^2 Z_d} \quad (4)$$

where m_d is the mass of a dust particle, for which we adopt here $5 \cdot 10^{-13}$ g, and Z_d is the charge of the typical dust particle. In Yan et al. (2004), the grain charge for carbon and silicon is discussed to become as large as $Z_d \sim 500$. We use this value as an upper limit. Dust is about 1 percent of the ISM, and so a PBH meets a dust particle every few million years, so about 50 times per orbit. This leads to a charge of about $Z_{BH} \approx 3 \cdot 10^4$. The limiting charge from stopping accretion is given by $Z_{BH} = 4 \cdot 10^{13}$, which is never reached, so gravitation always dominates over electric repulsion between PBH and charged dust. On the other hand, whenever such a dust charged PBH hits a star, then the effects could be dramatic. This is due to the fact, that then the PBH will be a perfect attractor for the opposite charge, with a strongly enhanced cross-section. But this happens, once again, only to very rare PBHs. So the charge of a PBH could become quite appreciable, in absolute terms, although never relevant, as it almost never hits a star. This implies, that the "typical" PBH might have a charge of up to order a few thousand, over the lifetime of the Galaxy. If that were really true, then the PBH would actually cancel its charge going through a dense star. But it would not be enough to actually slow it down appreciably, even then.

Our conclusions are that the charge itself will never be large enough to produce a significant effect compared to gravitational interactions. For charges as considered above, any rotational effect possibly present, see Casadio et al. (1997), will not play a significant role, since the induced magnetic fields are obviously too small.

3. Primordial black holes - constraints

Ever since the hypothesis of primordial black holes was first established (Hawking 1971), different methods for setting constraints on their actual abundance in the Universe were discussed. These methods divide into theoretical and observational constraints. While the former are rather speculative and model dependent (see e.g. Carr (2005); Khlopov (2008)), the latter are more robust and do constrain the abundance of primordial black holes in two mass ranges. In this section, we briefly review the current possibilities to observationally constrain PBH abundances and discuss how the search for PBH interactions with Galactic objects could help to further constrain the mass function of PBHs.

There are two main methods seeking the indirect detection of primordial black holes. The first one aims for the detection of PBH evaporation. This method is sensitive to the lower mass limit of the initial mass function (IMF). As predicted by Hawking (1974), and shortly later also by Bekenstein (1975), PBHs evaporate due to quantum fluctuations around the Schwarzschild radius of the black hole, leading to the evaporation of PBHs below $5 \cdot 10^{14}$ g until today. Thus, the non-detection of the high-energy photons, i.e. $E_\gamma \gtrsim 20$ MeV, leads to a robust constraint on the mass function around 10^{15} g. At 10^{15} g, EGRET observations between 30 MeV and 120 MeV imply that the PBH mass density must be smaller than $5.1 \cdot 10^{-9}$ times the total dark matter (Sreekumar et al. 1998). At higher mass scales (10^{26} g $<$ m_{pbh} $<$ 10^{33} g), micro-lensing can help to restrict the abundance of PBHs, see e.g. Afonso et al. (2003). The excluded regions for the mass function are shown in Fig. 1. In addition, it was proposed by Gould (1992) to use gamma ray bursts (GRBs) to detect “femto-lenses”, produced by dark matter objects in the mass range of 10^{17} g $<$ m_{pbh} $<$ 10^{20} g. This method has, however, not been applied so far and no experimental limit has been set yet. Hence, a mass range of about ten orders of magnitude, 10^{15} g $<$ m_{pbh} $<$ 10^{26} g, remains unexplored so far. In the standard scenario of density perturbations in the early Universe, the IMF of PBHs behaves as, e.g. Halzen et al. (1991)

$$IMF \propto m_{pbh}^{-2.5}. \quad (5)$$

Thus, most PBHs have masses at evaporation level. The constraint by EGRET at the lower end of the mass scale has therefore significant consequences for the abundance of black holes at higher masses. There are, however, proposed theories for PBH production at different mass scales, for example the collapse of topological defects, softening of the equation of state and quantum gravity scenarios, which, although speculative, deserve to be tested (see reviews by Carr (2005); Khlopov (2008) and references therein).

4. Interaction probability

The event rate of a primordial black hole striking a star is given as

$$\dot{n} \approx N_\star \cdot j_{pbh} \cdot \sigma_{pbh,\star}. \quad (6)$$

Here, N_* is the number of stars in the considered population. The flux of primordial black holes, \dot{j}_{pbh} , is given by multiplying the PBHs' number density n_{pbh} with their velocity v_0 :

$$\dot{j}_{pbh} = n_{pbh} \cdot v_0. \quad (7)$$

We use the rotational velocity as a measure for the PBH velocity, $v_0 \approx 2.2 \cdot 10^7 \text{ cm s}^{-1}$. The number density of primordial black holes can be estimated by assuming that PBHs represent a fraction η of the DM in the Galactic halo, $M_{DM} \approx 9 \cdot 10^{11} M_\odot$. The halo is spherical with an approximate radius of $r_{halo} \sim 50 \text{ kpc}$. We assume here that all PBHs are produced at the same mass value m_{pbh} and leave this as a free parameter. The number density of PBHs can then be written as

$$n_{pbh} = \frac{\eta \cdot M_{DM}}{4/3 \pi r_{halo}^3} \cdot \frac{1}{m_{pbh}}. \quad (8)$$

Hence, the event rate can be expressed as

$$\dot{n} \approx N_* \cdot \frac{\eta \cdot M_{DM}}{4/3 \pi r_{halo}^3} \cdot \frac{v_0}{m_{pbh}} \cdot \sigma_{pbh,*}. \quad (9)$$

The cross section of a PBH interacting with a star is given as

$$\sigma_{pbh*} = \pi R_0^2. \quad (10)$$

Here, we use the conservation of angular momentum in order to estimate the impact parameter R_0 , which guarantees the collision with the star. The PBH has an angular momentum of $m_{pbh} v_0 R_0$ at the limiting case of interaction, when approaching the star with an offset from the center corresponding to the impact parameter R_0 . This should be equal its angular momentum when arriving at the surface of the star, R_* :

$$v_0 R_0 = v_{\parallel} \cdot R_* \approx v_* \cdot R_* \quad (11)$$

with v_{\parallel} as the parallel component of the final PBH velocity $v_*^2 = v_{\parallel}^2 + v_{\perp}^2$. We assume $v_{\parallel} \approx v_*$ as the case of maximum angular momentum is the limiting case, less angular momentum will always result in collision if maximum angular momentum does. The calculation of the final velocity is done by considering energy conservation:

$$\frac{1}{2} v_0^2 - \frac{G M_*}{\langle R \rangle} = \frac{1}{2} v_*^2 - \frac{G M_*}{R_*} \quad (12)$$

with M_* as the mass of the star. The characteristic distance of the PBH entering the gravitational field of the star can be approximated as the typical distance between objects in the galaxy, assuming that each star-like objects deflects the PBH at least marginally. We assume this typical distance to be $\langle R \rangle \sim 1 \text{ pc}$. We find that the gravitational energy is negligible in the initial state¹, so that the final velocity can be expressed as

$$v_* \approx \sqrt{v_0^2 + \frac{2 G M_*}{R_*}} = \sqrt{v_0^2 + v_{esc}^2}. \quad (13)$$

¹For $\langle R \rangle = 1 \text{ pc}$, we get $G M_* / \langle R \rangle \approx 7000 \text{ cm s}^{-1}$

Using Equ. (13) in Equ. (11) results in the correlation

$$R_0 = R_\star \cdot \frac{v_\star}{v_0} = R_\star \cdot \frac{\sqrt{v_0^2 + v_{esc}^2}}{v_0}. \quad (14)$$

For compact objects like white dwarfs and neutron stars, the initial velocity is typically much smaller than the escape velocity. In this case, the final velocity is determined by the escape velocity, $v_\star \approx v_{esc}$. For less compact objects like Earth and main sequence stars, the escape velocity is close to or smaller than the initial velocity. In that case, the velocity is of the order of the initial velocity, $v_\star \approx v_0$. Replacing the impact parameter R_0 in Equ. (9) by using Equ. (14) yields

$$\dot{n} \approx N_\star \cdot \frac{\eta \cdot M_{DM}}{4/3 r_{halo}^3} \cdot \frac{v_0}{m_{pbh}} \cdot \left(\frac{v_\star}{v_0}\right)^2 \cdot R_\star^2 \quad (15)$$

$$= 2 \cdot 10^{-3} \text{yr}^{-1} \cdot N_{\star,9} \cdot \eta_1 \cdot v_{\star,0}^2 \cdot R_{\star,9}^2 \cdot m_{pbh,20}^{-1}. \quad (16)$$

Here, we use fixed numbers for the dark matter mass in the Galaxy, $M_{DM} = 9 \cdot 10^{11} M_\odot$ and for the halo radius, $r_{halo} = 50$ kpc. Other variables are $N_{\star,9} := N_\star/10^9$, $\eta_1 := \eta/1$, $v_{\star,0} := v_\star/v_0$, $R_{\star,9} := R_\star/(10^9 \text{cm})$ and $m_{pbh,20}/(10^{20} \text{g})$. Apart from the PBH mass, which we leave as a variable, the remaining parameters depend on the property of the astrophysical objects considered. For instance, white dwarfs ($v_\star/v_0 = 51/2.2$) have an event rate of 1.4 yr^{-1} for a black hole mass of 10^{20} g .

5. Energy deposit during the passage

In our estimate of the kinetic energy which is transferred from the black hole to the star and being radiated, we follow previous studies of motion of accretors in continuous medium, see e.g. Ruderman and Spiegel (1971). In this first estimate, we assume a uniform and frictionless medium and we disregard the fact that the gas is self-gravitating.

The black hole passing through the gas is focusing matter behind itself, creating a wake, because of the gravitational interaction transferring momentum to the atoms nearby. The inhomogeneity in the medium is the source of a force acting on the black hole, implying the decrease in kinetic energy.

As pointed out by Ostriker (1999), the force on the black hole and hence the energy loss depends on whether the motion is supersonic or not, as well as on the degree of supersonic motion. In first order approximation, we consider the motion of the black hole to be at constant speed. In addition, we assume the velocity to be supersonic, so that the drag force, and hence for the energy loss, reduces to the one presented in (Ruderman and Spiegel 1971). The bow shock is negligible compared to the tail shock's energy loss. Consequently, the energy loss per time is constrained to

$$\frac{dE}{dt} = \frac{4\pi G^2 m_{pbh}^2 \rho_\star}{v_\star} \ln \frac{r_{\max}}{r_{\min}}, \quad (17)$$

where r_{\max} is the maximal linear dimension of the star (i.e. its diameter), r_{\min} is the linear dimension of the accretor, lying between the black hole horizon and the Bondi-Hoyle radius of the black hole. The exact formulation of the linear scales is not crucial for this first estimate, as they appear in a logarithm. Here, we use $\ln(r_{\max}/r_{\min}) = 10$. The total energy loss is then given as

$$E = \frac{dE}{dt} \cdot dt = \frac{8\pi G^2 m_{pbh}^2 R_\star \rho_\star}{v_\star^2} \ln \frac{r_{\max}}{r_{\min}}, \quad (18)$$

considering a passage time of $dt \approx 2 \cdot R_\star/v_\star$. Equation (18) can be expressed as

$$E = 2 \cdot 10^{27} \text{ erg} \cdot m_{pbh,20}^2 \cdot R_{\star,9} \cdot v_{\star,0}^{-2} \cdot \rho_{\star,5}. \quad (19)$$

Here, $\rho_{\star,5} := \rho_\star/(10^5 \text{ g cm}^{-3})$. Table 2 lists the energy released and the interaction probability for black holes of 10^{20} g passing through the different Galactic objects.

In our picture, the shock front will locally heat the plasma depending on the particular Galactic object under consideration. The spectrum is therefore a thermal one. In the following, the peak energy of the spectrum is discussed in order to estimate the detectability in detector systems observing in the relevant energy range.

To compute the temperature of the shock, we assume supersonic shock conditions and a perfect gas with the result

$$T_S = \frac{5}{64} \frac{m_H}{k_B} v_\star^2 M^2 > 4.5 \cdot 10^5 \text{ K} \cdot v_{\star,0}^2, \quad (20)$$

where the downstream velocity is diminished by a factor four with respect to the upstream velocity, e.g. (Landau and Lifshitz 1987; Parks 1991). Here, k_B is the Boltzmann constant, v_\star is the velocity of the shock, m_H is the mass of a hydrogen atom, M is the Mach number, $2.2 \cdot 10^7 \text{ cm s}^{-1}$ is the assumed average relative velocity between primordial black holes and stars. Wien's law now yields the frequency at maximum intensity as

$$\nu_{\max} = \frac{c T_S}{b} = \frac{c}{b} \cdot \frac{5}{64} \frac{m_H}{k_B} v_\star^2 \left(\frac{M}{1}\right)^2 > 4.5 \cdot 10^{16} \text{ Hz} \cdot v_{\star,0}^2, \quad (21)$$

with $b = 2.9 \cdot 10^{-3} \text{ Km}$. The peak can also be expressed in term of peak photon energy

$$E_{\text{peak}} = h\nu_{\max} > 0.2 \text{ keV} \cdot v_{\star,0}^2. \quad (22)$$

This peak energy is merely lower limit, but should suffice as a first-order estimate. In case of a collision with Earth, an extreme ultraviolet spectrum is expected. For main sequence stars and red giant cores result in X-ray spectra. White dwarfs and neutron stars cannot be treated with simple thermodynamics. We here assume that the shock velocity v_\star determines the temperature of the shock with $E_{\text{peak}} = 0.8 \text{ keV} \cdot v_{\star,0}^2$. For a white dwarf, we get a soft γ spectrum, while for a neutron star we end up in high-energy gamma rays, see table 2.

6. Signatures and detectability

The events discussed above are detectable if two conditions are met:

1. *a single event is strong enough to be seen by a detector;*
2. *the events are frequent enough so that they can be seen within the detector's life time.*

In this section, the two criteria are examined quantitatively for different detectors, observing in the energy range of the expected signal.

6.1. Detector sensitivity and photon fluence

To investigate whether or not the above energy release of a single event is sufficient for detection at Earth, it is necessary to consider the photon fluence at Earth, F_γ , depending on the event's distance from Earth, d ,

$$F_\gamma = \frac{E}{\Omega \cdot (1+z) \cdot d^2} \approx \frac{E}{\Omega \cdot d^2}. \quad (23)$$

The redshift factor $(1+z)$ describes adiabatic energy losses, which can be neglected on Galactic scales, $z \approx 0$. The opening angle of the emitted signal Ω is determined by the shape of the shock. For a significant signal, the flux must exceed the sensitivity of the detector F_{sens} ,

$$F_\gamma \geq F_{sens}. \quad (24)$$

A detector's sensitivity is limited by the detection of a single photon of energy E_γ ,

$$F_{sens} = \frac{E_\gamma}{A_{eff}} \quad (25)$$

assuming there is no additional background. A single photon can be significant if the background is as much smaller than unity, see also Biermann et al. (1981). As soon as there is some significant background, more than one photon will be needed for detection. We use this single photon argument as an absolute upper limit of the signal to be detected. Here, A_{eff} is the effective area of the detector. Combining Equations (23), (24), and (25), we have

$$\frac{E}{\Omega \cdot d^2} \geq \frac{E_\gamma}{A_{eff}}. \quad (26)$$

Typically, the effective detection area A_{eff} depends on the energy E_γ of detection and the detector is sensitive to the shape of the spectrum. Here, we conservatively assume that the effective area is concentrated at the lower energy threshold of the detector. For higher energies, the sensitivity would be less. For a given detector, the maximum distance for an event to be observed can be evaluated as

$$d_{\max} = \sqrt{\frac{E}{E_\gamma} \cdot \frac{A_{eff}}{\Omega}}. \quad (27)$$

Inserting the total energy released as presented in Equ. (19) yields

$$d_{\max} = 6.6 \text{ pc} \cdot m_{pbh,20} \cdot R_{\star,9}^{1/2} \cdot v_{\star,0}^{-1} \cdot \rho_{\star,5}^{1/2} \cdot A_{eff,2500}^{1/2} \cdot \Omega_{4\pi}^{-1/2} \cdot E_{\gamma,1.5}^{-1/2}, \quad (28)$$

with an absolute maximum of $d_{\max} \leq d_{\text{Galaxy}}$. The effective area reference value $A_{eff,2500} := A_{eff}/(2500 \text{ cm}^2)$, corresponds to XMM Newton properties, at a reference energy of $E_{\gamma,1.5} := E_{\gamma}/(1.5 \text{ keV})$. The opening angle of the signal is expressed in terms of the maximum opening angle, corresponding to a isotropically emitted signal, $\Omega_{4\pi} := \Omega/(4\pi)$.

6.2. Observation time and interaction probability

To estimate whether the event rate is sufficiently high, we can evaluate the observation time t_{obs} needed in order to have a number of N events occurring within a distance d from Earth:

$$N = \dot{n}(d) \cdot \frac{\Omega_{obs}}{4\pi} \cdot \frac{\Omega}{4\pi} \cdot t_{obs}. \quad (29)$$

The solid angle Ω_{obs} describes the detector's Field of View (FoV). The solid angle Ω accounts for a possibly beamed signal, which reduces the total number of events to be observed, since only a fraction $\Omega/(4\pi)$ is directed towards Earth. The total event rate \dot{n} in the Galaxy was determined in Section 4. Since the observation of the signal is limited by its strength as suggested in the previous subsection, a smaller volume, dependent on the distance $d = d_{\max}$ is observed. The event rate scales down with the volume containing the astrophysical objects:

$$\dot{n}(d_{\max}) = \frac{V(d_{\max})}{V_{tot}} \cdot \dot{n}. \quad (30)$$

with $d_{\max} \leq d_{\text{Galaxy}}$. In the following calculations we use the approximation that the majority of stars and other astrophysical objects are distributed along the Galactic disk, and ignore the spheroidal population for the purpose of this estimate.

$$V(d_{\max}) = \pi d_{\max}^2 h, \quad (31)$$

with h as the thickness of the Galaxy. The total volume of the Galactic disk is

$$V_{tot} = \pi d_{\text{Galaxy}}^2 h, \quad (32)$$

with $d_{\text{Galaxy}} \approx 15 \text{ kpc}$ as the radius of the Galaxy. We use the optimistic assumption that the entire thickness of the Galactic disk $h \approx 300 \text{ pc}$ is visible. Therefore, the number of N events within a radius $d_{\max} \leq d_{\text{Galaxy}}$ is

$$N = \dot{n} \cdot \left(\frac{\min(d_{\max}, d_{\text{Galaxy}})}{d_{\text{Galaxy}}} \right)^2 \cdot \frac{\Omega_{obs}}{4\pi} \cdot \frac{\Omega}{4\pi} \cdot t_{obs}. \quad (33)$$

For the detection of a single event, $N = 1$, the required observation time is given as

$$t_{obs} = 1 \text{ yr} \cdot \frac{4\pi}{\Omega_{obs}} \cdot \frac{4\pi}{\Omega} \cdot \left(\frac{\dot{n}}{1 \text{ yr}^{-1}} \right)^{-1} \cdot \left(\frac{\min(d_{\max}, d_{\text{Galaxy}})}{d_{\text{Galaxy}}} \right)^{-2}. \quad (34)$$

Combining Equations (16), (28), and (34) yields

$$t_{obs}(m_{pbh} < m_{pbh}^{\text{break}}) = 3.5 \cdot 10^{11} \text{ yr} \cdot m_{pbh,20}^{-1} \cdot R_{\star,9}^{-3} \cdot \rho_{\star,5}^{-1} \cdot N_{\star,9}^{-1} \cdot \Omega_{4\pi}^{-1} \cdot \eta_1^{-1} \cdot A_{eff,2500}^{-1} \cdot \Omega_{obs,0.2}^{-1} \cdot E_{\gamma,1.5} \quad (35)$$

for $d_{\text{max}} < d_{\text{Galaxy}}$ and

$$t_{obs}(m_{pbh} \geq m_{pbh}^{\text{break}}) = 5 \cdot 10^2 \text{ yr} \cdot \Omega_{obs,0.2}^{-1} \cdot \Omega_{4\pi}^{-1} \cdot N_{\star,9}^{-1} \cdot \eta_1^{-1} \cdot m_{pbh,20} \cdot v_{\star,0}^{-2} \cdot R_{\star,9}^{-2} \quad (36)$$

for $d_{\text{max}} = d_{\text{Galaxy}}$. Here, $\Omega_{obs,0.2} := \Omega_{obs}/(0.2 \text{ sr})$.

This break in the function $t_{obs}(m_{pbh})$ happens at masses of

$$m_{pbh}^{\text{break}} = 4.5 \cdot 10^{23} \text{ g} \cdot R_{\star,9}^{-1/2} \cdot v_{\star,0} \cdot \rho_{\star,5}^{-1/2} \cdot \Omega_{4\pi}^{1/2} \cdot A_{eff,2500}^{-1/2} \cdot E_{\gamma,1.5} \quad (37)$$

The observation time reaches its minimum at this break mass.

6.3. Detectability

In Section 5, it was discussed that a signal at X-ray energies is expected. We choose four detectors currently in operation, which are well-suited due to their relatively large FoVs and effective areas: We examine our results for XMM NEWTON, because this detector is sensitive at extreme UV to X-rays. We use XMM Newton’s effective area as quoted in XMM-web at the reference energy 1.5 keV. The results we obtain are equivalent to what is expected from observations with Chandra. For higher energies, hard X-rays to soft gamma-rays, we use SWIFT-BAT and FERMI-GBM as reference detectors. Swift covers the range between 15 keV and 150 keV, the high-energy detector of the GBM covers the energy range 150 keV to 30 MeV. Both instruments provide quite large effective areas in combination with a large FoV, as they are designed to detect GRBs. For high-energy radiation, we use Fermi-LAT parameters, covering 20 MeV up to 300 GeV. Table 3 summarizes the properties of the four detectors. For Swift and Fermi, we use the lower energy threshold as the reference energies for the effective areas quoted in Swift-web; Fermi-web. This is the most optimistic approach, since using higher energies would lead to reduced sensitivities.

The detector’s effective area, FoV and energy determines then the observation time as well as the break masses as discussed in the previous subsection. It turns out that the observation times for the four different detectors are correlated as

$$t_{obs}^{\text{XMM}} = 2 \cdot t_{obs}^{\text{Swift/BAT}} = 0.2 \cdot t_{obs}^{\text{Fermi/GBM}} = 0.003 \cdot t_{obs}^{\text{Fermi/LAT}} \quad (38)$$

and the break mass m_{pbh}^{break} are connected as

$$m_{pbh}^{\text{break, XMM}} = 2 \cdot m_{pbh}^{\text{break, Swift/BAT}} = 0.1 \cdot m_{pbh}^{\text{break, Fermi/GBM}} = 0.02 \cdot m_{pbh}^{\text{break, Fermi/LAT}}. \quad (39)$$

Thus, Swift/BAT provides the shortest and therefore best option concerning observation times. Fermi/LAT provides the largest break mass. Figure 2 shows the observation time versus PBH mass for the case of XMM Newton in the relevant mass range of $10^{15} \text{ g} < m_{pbh} < 10^{26} \text{ g}$. Masses outside of this range are already proved not to contribute significantly ($< 10\%$) to the dark matter. The solid line represents main sequence stars, the dashed line shows red giant cores, the dotted line is the result for white dwarfs and the dot-dashed line displays neutron stars. The shortest observation times are achieved for main sequence stars, and even here, the best case at $m_{pbh} = 2 \cdot 10^{24} \text{ g}$ requires observation times of more than 100 years. Similar results are achieved for Swift, Fermi-GBM and Fermi-LAT, as shown in Figures 3, 4 and 5, where the observation times need to be larger than 100 years as well in order to see one event, except in the case of Fermi/GBM at $3 \cdot 10^{25} \text{ g}$, where 60 years suffice. The best observation times t_{obs}^{best} are achieved for the break in the observation time function versus PBH masses m_{pbh}^{break} . They are listed for the four detectors in Table 3.

The observation times lie far above what is provided during the lifetime of the presented detectors. Given that our calculations should be considered as an upper limit to what can be expected in reality, we conclude that the detection of PBH interactions with Galactic objects can be excluded due to too small event rates in combination with an extremely small energy release.

6.4. Alternative signatures

There are a few other processes that could in principle lead to the production of a detectable signal for different detectors. We will briefly discuss here, why these mechanisms fail to produce a significant signal:

- *Shock acceleration of charged particles*

Particles can gain energy by scattering off magnetic inhomogeneities through the concept of stochastic acceleration (Fermi 1949, 1954). However, inside of the stars, the density is extremely high, and for white dwarfs and neutrons stars the matter is degenerate. The mean free path of a proton in matter can be determined by considering the total cross section for proton-proton interactions, $\sigma_{pp} \approx 50 \text{ mbarn}$:

$$\lambda_{mfp} = \frac{m_p}{\rho_{\star} \cdot \sigma_{pp}} = 3 \cdot 10^{-4} \text{ cm} \cdot \rho_{\star,5}. \quad (40)$$

The mean free path is typically smaller than a centimeter and does not allow for significant acceleration. Injection and acceleration of energetic charged particles in shock fronts is therefore highly disfavored, with the possible exception of the tenuous envelopes of red giant stars.

- *Star quakes*

PBHs passing through an astrophysical object can induce star quakes. Although the emitted photons themselves cannot be distinguished from the general thermal spectrum of the star,

it can be detected by Fourier-transforming the spectrum from time to frequency space, see (Donea et al. 1999; Martínez-Oliveros et al. 2007, e.g.) and references therein. However, those quakes can so far only be detected on the sun. The probability of an interaction with the sun is 10^{-7} yr^{-1} . Interactions with the sun can therefore be excluded as a possible signal.

7. Conclusions

We showed in the previous section that the process of dynamical friction cannot lead to a detectable signal with current instruments: we calculated a lower limit for the observation time for most suited detectors, XMM Newton, Swift-BAT, and Fermi-GBM and Fermi-LAT. This lower limit is based on the assumptions that

- *The entire energy loss is radiated at the produced wavelength without significant delays,*
- *one photon suffices for a significant detection of a signal,*
- *all energy is contained in the detector’s energy range,*
- *the entire thickness of the Galactic disk can be observed,*
- *the signal is emitted isotropically.*

All assumptions are in favor of detection, more realistic settings will reduce the detectability even more. We investigate interactions with main sequence stars, red giants, white dwarfs, and neutron stars. Independent of the class of objects, the difficulty is that either the total energy loss of the process is too low (small masses around $10^{15} \text{ g} < m_{pbh} < 10^{20} \text{ g}$) or the event rate is too small (large masses around $10^{20} \text{ g} < m_{pbh} < 10^{26} \text{ g}$). Even with the optimistic assumptions listed above, observation times of at least 60 years are required in order to see a single event for all objects and all detectors considered.

Although we use average values for both mass and velocity distribution of PBHs, fluctuations from those central values will not influence the result of these calculations significantly. One could, for instance, argue that the clumping of dark matter as discussed by Binney and Tremaine (2008) would lead to an enhanced signal. However, such an effect would need to increase the event rate by at least a factor 10^2 to achieve reasonable observation times of $t_{obs} < 1 \text{ yr}$. The only possibility of such an enhancement is in the central bulge of the galaxy (Navarro et al. 1997), where the density is assumed to peak with an r^{-1} decrease from the center. However, due to the high activity in the Galactic center, the background will be too high to distinguish a PBH interaction from standard processes or other dark matter signatures.

Hence, we conclude that constraining the abundance of PBHs in DM using interactions of PBHs with Galactic objects is not possible in the standard scenario described above. A significant rate of GRB-like events as suggested in (Zhilyaev 2007) can therefore be excluded. There may be

additional effects, like the clumping of dark matter, the observation of nearby dwarf galaxies or the density spike in the galactic center, leading to an enhanced event rate and energy release. Still, these will have to be able to improve the observation times in this standard scenario by at least a factor 100 in order to have a visible signal. The main reason is that observation times of a few months may be available from the different telescopes, but not more.

In addition, the probability for a PBH colliding with Earth is as low as $10^{-12} \text{ yr}^{-1} \cdot m_{pbh,20}^{-1}$. This means less than one event each $10^{7 \rightarrow 17}$ years of such a kind is expected. The interpretation of the Tungus event as a collision with a PBH, see Jackson and Ryan (1973), can therefore be excluded as well.

We would like to thank Alina Donea, Maxim Khlopov and Wlodek Bednarek for helpful discussions. MAA acknowledges the support from the Polish Ministry of Science, grant N203 0093/1466, and from the Swedish Research Council, grant VR Dnr 621-2006-3288. JKB is supported by the Deutsche Forschungsgemeinschaft (DFG), grant BE-3712/3-1. Support for work with PLB comes from the AUGER membership and theory grant 05 CU 5PD 1/2 via DESY/BMBF and from VIHROS. AG acknowledges the support from the Knut and Alice Wallenberg Foundation. For LQ, support is coming from the Chinese Scholarship Council. Further acknowledgments go to Nordita for traveling grants for MAA, JKB and FJ.

REFERENCES

- C. Afonso et al. *A&A*, 400:951, 2003.
- J. D. Bekenstein. *Phys. Rev. D*, 12:3077, 1975.
- G. Bertone, D. Hooper, and J. Silk. *Phys. Rep.*, 405:279, 2005.
- P. Biermann and M. Harwit. *Astroph. Journal Let.*, 241:L105, 1980.
- P. L. Biermann and A. Kusenko. *Phys. Rev. Let.*, 96(9):091301, 2006.
- P. L. Biermann et al. *Astroph. Journal Let.*, 247:53, 1981.
- J. Binney and S. Tremaine. *Galactic Dynamics: Second Edition*. Princeton University Press, Princeton, NJ USA, 2008.
- H. Bondi and F. Hoyle. *MNRAS*, 104, 1944.
- B. J. Carr. *ArXiv:astro-ph/0504034 (preprint)*, 2005.
- R. Casadio et al. *Phys. Rev. D*, 55:814, 1997.
- A.-C. Donea, D. C. Braun, and C. Lindsey. *Astroph. Journal Let.*, 513:L143, 1999.
- E. Fermi. *Phys. Rev.*, 75(8):1169, 1949.
- E. Fermi. *ApJ*, 119:1, 1954.
- Fermi-web. <http://fermi.gsfc.nasa.gov/>, 2008. Fermi web-page.
- A. Gould. *Astroph. Journal Let.*, 386:L5, 1992.
- H. E. Haber and G. L. Kane. *Phys. Rep.*, 117:75, 1985.
- F. Halzen et al. *Nature*, 353:807, 1991.
- S. W. Hawking. *MNRAS*, 152:75, 1971.
- S. W. Hawking. *Nature*, 248:30, 1974.
- D. Hooper and S. Profumo. *Phys. Rep.*, 453:29, 2007.
- A. A. Jackson and M. P. Ryan. *Nature*, 245:88, 1973.
- F. D. Kahn and L. Woltjer. *ApJ*, 130:705, 1959.
- M. Y. Khlopov. *ArXiv:0801.0116 (preprint)*, 2008.
- E. Komatsu et al. *ArXiv: 0803.0547 (preprint)*, 2008. Submitted to ApJ Supp. Series.

- L. D. Landau and E. M. Lifshitz. *Course of Theoretical Physics, Vol.6 : Fluid Mechanics*. Butterworth-Heinemann, 2nd edition, 1987.
- J. C. Martínez-Oliveros et al. *Solar Physics*, 245:121, 2007.
- J. S. Mathis, W. Rumpl, and K. H. Nordsieck. *ApJ*, 217:425, 1977.
- J. F. Navarro, C. S. Frenk, and S. D. M. White. *ApJ*, 490:493, 1997.
- E. C. Ostriker. *ApJ*, 513:252, 1999.
- J. P. Ostriker, P. J. E. Peebles, and A. Yahil. *Astroph. Journal Let.*, 193:L1, 1974.
- G. K. Parks. *Physics of space plasmas*. Addison-Wesley Publishing Company, 1991.
- M. A. Ruderman and E. A. Spiegel. *ApJ*, 165:1, 1971.
- P. Sreekumar et al. *ApJ*, 494:523, 1998.
- Swift-web. <http://swift.gsfc.nasa.gov/docs/swift/swiftsc.html>, 2008. Swift web-page.
- XMM-web. <http://heasarc.nasa.gov/W3Browse/all/xms.html>, 2008. XMM Newton web-page.
- X. Xue et al. *ArXiv:0801.1232 (preprint)*, 2008. accepted by ApJ.
- H. Yan, A. Lazarian, and B. T. Draine. *ApJ*, 616:895, 2004.
- J. Yoo, J. Chaname, and A. Gould. *A&A*, 601:311, 2004.
- B. E. Zhilyaev. *Bulletin Crimean Astrophysical Observatory*, 103:58, 2007. arXiv:0706.0930.
- F. Zwicky. Die Rotverschiebung von extragalaktischen Nebeln. *Helvetica Physica Acta*, 6:110, 1933.
- F. Zwicky. *ApJ*, 86:217, 1937.

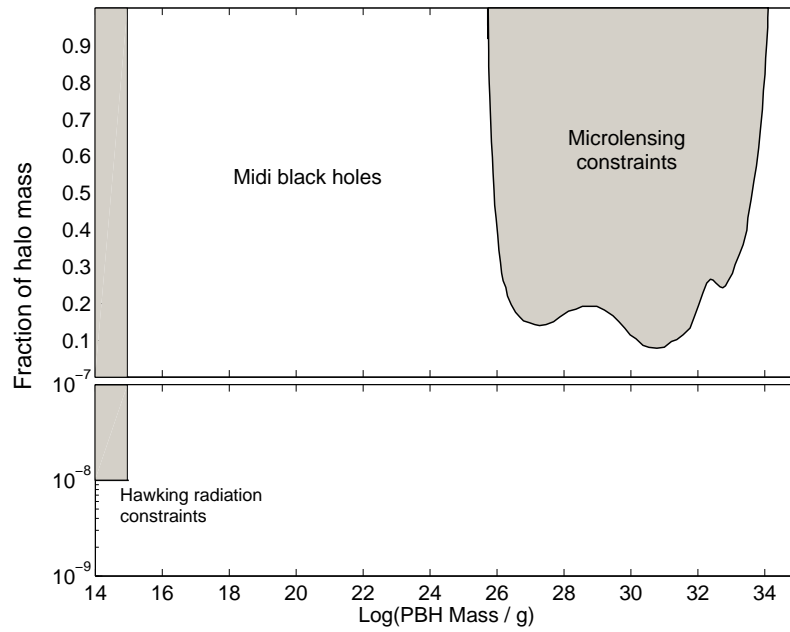


Fig. 1.— Mass regions excluded by evaporation signatures (Sreekumar et al. 1998), $\sim 10^{15}$ g, and by micro-lensing (Afonso et al. 2003), 10^{26} g $< m_{pbh} < 10^{33}$ g.

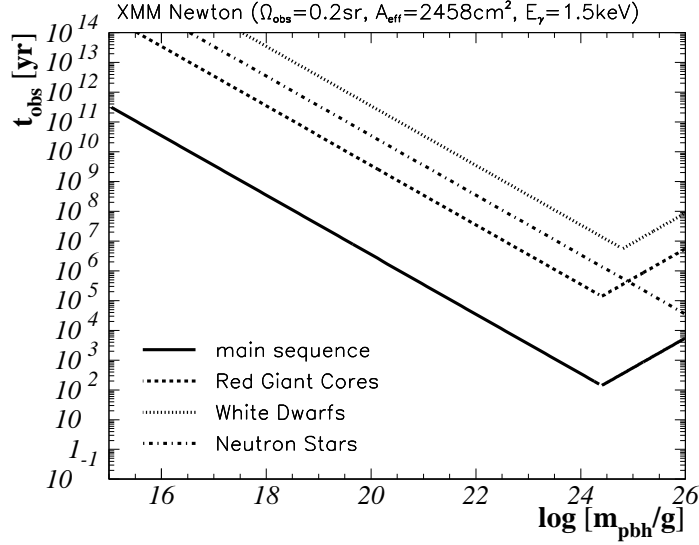


Fig. 2.— Observation time of PBH interactions with Galactic objects, observing with XMM Newton. Solid line: main sequence stars; dashed line: red giant cores; dotted line: white dwarfs; dot-dashed line: neutron stars. The observation time decreases with m_{pbh}^{-1} , until the point where the entire Galaxy can be observed and it starts increasing with m_{pbh} .

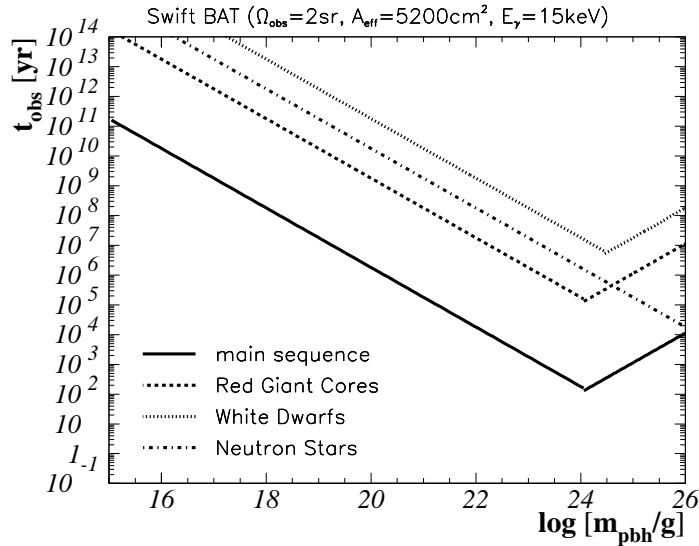


Fig. 3.— Observation time of PBH interactions with Galactic objects, observing with Swift-BAT. Same representation as in Fig. 2.

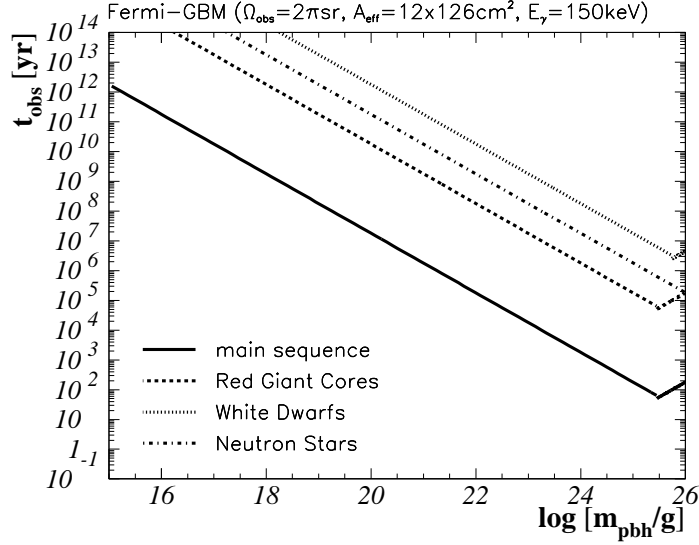


Fig. 4.— Observation time of PBH interactions with Galactic objects, observing with Fermi-GBM. Same representation as in Fig. 2.

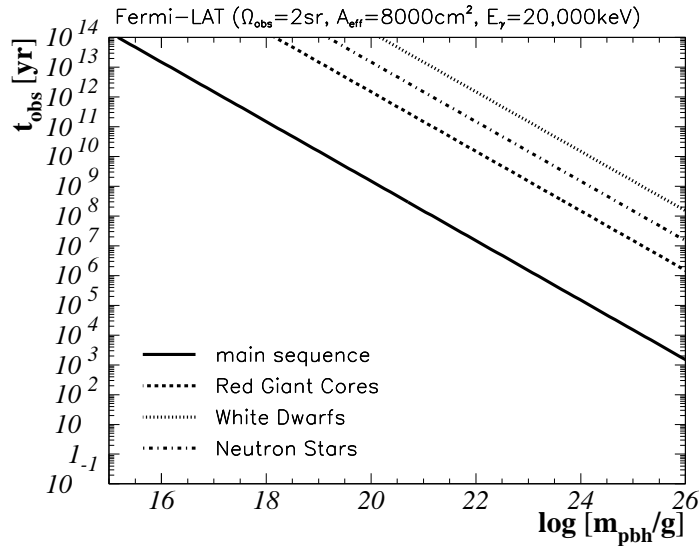


Fig. 5.— Observation time of PBH interactions with Galactic objects, observing with Fermi-LAT. Same representation as in Fig. 2.

Table 1. Basic properties of objects considered for collisions with primordial black holes.

		Earth	main sequ. stars	red giant cores	white dwarfs	neutron stars
number in MW	N_\star	1	10^{11}	10^9	10^9	10^9
mass	M_\star/M_\odot	$3 \cdot 10^{-6}$	1	1	1	1
radius	R_\star [cm]	$6.4 \cdot 10^8$	10^{11}	10^{10}	10^9	10^6
density	ρ_\star [g cm $^{-3}$]	5.5	100	$10^{4 \rightarrow 5}$	$10^{5 \rightarrow 6}$	$10^{13 \rightarrow 15}$

Table 2. Energy loss according to Ruderman and Spiegel (1971) for a PBH mass of $m_{pbh} = 10^{20}$ g. The energy loss rate scales with $(m_{pbh}/10^{20}\text{g})^2$. The interaction probability \dot{n} scales with $(m_{pbh}/10^{20}\text{g})^{-1}$.

$m_{pbh} = 10^{20}$ g	Earth	main sequ. stars	red giant cores	white dwarfs	neutron stars
v_\star [cm s $^{-1}$]	$2.2 \cdot 10^7$	$5.5 \cdot 10^7$	$1.6 \cdot 10^8$	$5.1 \cdot 10^8$	$1.6 \cdot 10^{10}$
dE/dt [erg s $^{-1}$]	$1.5 \cdot 10^{21}$	10^{22}	$3 \cdot 10^{23 \rightarrow 24}$	$10^{24 \rightarrow 25}$	$3 \cdot 10^{30 \rightarrow 32}$
dt [s]	60	3600	120	3.9	$1.2 \cdot 10^{-4}$
$dE/dt \cdot dt$ [erg]	$9 \cdot 10^{22}$	$4 \cdot 10^{25}$	$4 \cdot 10^{25 \rightarrow 26}$	$4 \cdot 10^{24 \rightarrow 25}$	$4 \cdot 10^{26 \rightarrow 28}$
E_{peak} [keV]	0.2	1	11	400	$4 \cdot 10^5$
\dot{n} [yr $^{-1}$]	$8 \cdot 10^{-13}$	$1.3 \cdot 10^4$	11	1.4	$1.1 \cdot 10^{-3}$

Table 3. Detector properties in the X-ray to soft gamma-ray range. In order to have an upper limit on the sensitivity, the lower energy threshold is used as E_γ in the case of Swift and Fermi. For XMM Newton, the reference energy $E_\gamma = 1.5$ keV was explicitly given for the listed effective area.

	XMM Newton (XMM-web)	Swift BAT (Swift-web)	Fermi GBM (Fermi-web)	Fermi LAT (Fermi-web)
$E_{\min}; E_{\max}$ [keV]	(0.1; 15)	(15; 150)	(10; 30000)	(20000; $3 \cdot 10^8$)
E_γ [keV]	1.5	15	150	20,000
Ω_{obs} [sr]	0.20	2	$\sim 2\pi$	2
A_{eff} [cm ²]	2485	5200	12×126	8000
main seq. stars				
m_{pbh}^{break} [g]	$3 \cdot 10^{24}$	$1 \cdot 10^{24}$	$3 \cdot 10^{25}$	$2 \cdot 10^{26}$
t_{obs}^{best} [yr]	140	140	60	750
Red Giant Cores				
m_{pbh}^{break} [g]	$3 \cdot 10^{24}$	$1 \cdot 10^{24}$	$3 \cdot 10^{25}$	$2 \cdot 10^{26}$
t_{obs}^{best} [yr]	$1.4 \cdot 10^5$	$1.4 \cdot 10^5$	$6.0 \cdot 10^4$	$7.5 \cdot 10^5$
White Dwarfs				
m_{pbh}^{break} [g]	$6 \cdot 10^{24}$	$3 \cdot 10^{24}$	$6 \cdot 10^{25}$	$4 \cdot 10^{26}$
t_{obs}^{best} [yr]	$5.5 \cdot 10^6$	$5.7 \cdot 10^6$	$2.4 \cdot 10^6$	$3.8 \cdot 10^7$
Neutron Stars				
m_{pbh}^{break} [g]	$3 \cdot 10^{26}$	$1 \cdot 10^{26}$	$3 \cdot 10^{27}$	$2 \cdot 10^{28}$
t_{obs}^{best} [yr]	$1.4 \cdot 10^4$	$1.4 \cdot 10^4$	$6.0 \cdot 10^3$	$7.5 \cdot 10^6$